Larsen, H.C., Duncan, R.A., Allan, J.F., Brooks, K. (Eds.), 1999
Proceedings of the Ocean Drilling Program, Scientific Results, Vol. 163

14. *DATA REPORT:* MASS ACCUMULATION RATES AND COMPOSITION OF NEOGENE ICE-RAFTED DEBRIS, SITE 919, IRMINGER BASIN[1]

Lawrence A. Krissek[2]

INTRODUCTION

At mid- to high-latitude marine sites, ice-rafted debris (IRD) is commonly recognized as anomalously coarse-grained terrigenous material contained within a fine-grained hemipelagic or pelagic matrix (e.g., Conolly and Ewing, 1970; Ruddiman, 1977; Krissek, 1989; Jansen et al., 1990; Bond et al., 1992; Krissek, 1995). The presence of such ice-rafted material is a valuable indicator of the presence of glacial ice at sea level on an adjacent continent, whereas the composition of the IRD can often be used to identify the location of the source area (e.g., Goldschmidt, 1995).

Because the amount of core recovered during Leg 163 was very limited, this shore-based, postcruise study focuses on materials recovered at a nearby site during Leg 152. In particular, this study examines sediments recovered at Site 919; these sediments were described as containing a significant ice-rafted component in the Leg 152 *Initial Reports* volume (Larsen, Saunders, Clift, et al., 1994). In this study, the sedimentary section from Site 919 has been examined with the goal of providing a detailed history of glaciations on Greenland and other landmasses adjacent to the Norwegian-Greenland Sea; this history ultimately will be calibrated using an oxygen isotope stratigraphy (Flower, 1998), although that calibration has not been completed at this time. Because ice-core studies of the Greenland Ice Sheet (GIS) have shown that the GIS changed dramatically, and in some cases extremely rapidly, during at least the last interglacial stage (GRIP Members, 1993), a detailed IRD record from the Southeast Greenland margin should provide insight into the longer term behavior of this sensitive component of the Northern Hemisphere climate system.

MATERIALS AND METHODS

The objective of this study was to generate records of the mass accumulation rate (MAR) and lithologic composition of coarse sand-sized IRD deposited at Site 919 during the past 960 k.y. Samples were taken from the Site 919 cores at a spacing of ~50 cm, providing a temporal resolution of ~3–5 k.y. Samples were specifically chosen to avoid discrete ash layers and possible coarse-grained turbidites. The age of each sample was calculated using the sample's subbottom depth and the sedimentation rates derived from shipboard biostratigraphic and magnetostratigraphic data (Larsen, Saunders, Clift, et al., 1994), supplemented by the preliminary oxygen isotope stratigraphy of Flower (1998).

Samples were processed to provide both compositional and MAR data. In order to calculate the MAR of coarse sand-sized IRD for each sample, the concentration (in weight percent) of the coarse-sand IRD within the total sediment was determined as follows:

1. The sample was dried at 60°C and weighed.
2. The sample was disaggregated in an ultrasonic bath, sieved at 250 µm and 2 mm to separate the coarse-sand fraction, and the coarse-sand fraction was weighed. The abundance of the coarse sand-size fraction (wt%) was then calculated using the weight of the total coarse-sand fraction and the initial dry sample weight.
3. The coarse-sand fraction was inspected through a binocular microscope to estimate the relative abundances of three grain types: IRD, biogenic components (radiolarians and foraminifers), and volcanic ash. In this examination, all coarse sand-sized grains that were not obviously either biogenic in origin or volcanic ash were assumed to be terrigenous IRD.
4. The weight percent of terrigenous coarse sand-sized IRD was calculated as the product of the weight percent of the total coarse-sand fraction and the relative abundance of IRD within the coarse-sand fraction. Visual inspection revealed that the majority of these samples are dominated by one grain type (i.e., either IRD, biogenic components, or volcanic ash). As a result, the temporal pattern of IRD importance could be illustrated without isolating IRD grains from samples with mixed grain populations. If more samples had contained such intermediate mixtures, however, the IRD would have been extracted by the appropriate use of chemical treatments (acid dissolution of carbonate and base dissolution of opal) and/or density separations (using sodium polytungstate).

The MAR of coarse sand-sized IRD for each sample was calculated as follows:

$$\text{IRD MAR} = (\%\text{CS} \times \%\text{T}) \times \text{LSR} \times \text{DBD},$$

where

1. (%CS × %T) is the product of the weight percent of the total coarse sand-size fraction and the relative abundance of IRD within the coarse sand-size fraction (thereby giving the weight percent of terrigenous coarse sand-sized IRD in the total sample, as described above) at a particular level.
2. LSR is the linear sedimentation rate in that interval. Linear sedimentation rates were determined from shipboard biostratigraphic and magnetostratigraphic data (presented in Larsen, Saunders, Clift, et al., 1994), and were refined using the preliminary oxygen isotope stratigraphy of Flower (1998).
3. DBD is the dry bulk density of that interval (taken as the value from the nearest shipboard index properties sample).

The values used in this calculation for each sample, as well as the resulting IRD MAR values, are given in Table 1.

The composition of the IRD was determined by visual examination using a binocular microscope. If a sample contained >100 grains of IRD, then the compositions of 100 grains were used to calculate the abundances of the various grain types; if a sample contained <100

[1]Larsen, H.C., Duncan, R.A., Allan, J.F., Brooks, K. (Eds.), 1999. *Proc. ODP, Sci. Results*, 163: College Station, TX (Ocean Drilling Program).
[2]Department of Geological Sciences, Ohio State University, Columbus, OH 43210, U.S.A. krissek@mps.ohio-state.edu

Table 1. Basic data, total mass accumulation rates of coarse sand-size ice-rafted debris, and mass accumulation rates for specific lithologies of coarse sand-size ice-rafted debris for samples from Site 919.

Site	Hole	Core	Type	Section	Top (cm)	Bottom (cm)	Depth (mbsf)	Age (ka)	%CS (wt% of coarse-sand fraction in total sample)	%Terrigenous grains in total coarse-sand fraction	Sed Rate (cm/k.y.)	DBD (g/cm^3)	IRD MAR (g/cm^2/k.y.)	CS %Qtz (quartz abundance in terrigenous coarse-sand fraction)	Qtz MAR (g/cm^2/k.y.)	CS %Bslt (basalt abundance in terrigenous coarse-sand fraction)
919	A	1	H	1	55	57	0.55	3.78	0.04	40	14.55	0.61	0.001	65	0	17
919	A	1	H	1	100	102	1	6.87	0.20	13	14.55	0.78	0.002	79	0.002	16
919	A	1	H	1	144	146	1.44	9.89	5.92	66	14.55	0.78	0.443	66	0.292	2
919	A	1	H	2	51	53	2.01	13.81	1.16	24	14.55	0.83	0.033	93	0.031	0
919	A	1	H	2	99	101	2.49	17.11	0.49	53	14.55	0.83	0.031	79	0.025	9
919	A	1	H	2	140	142	2.9	19.93	1.24	8	14.55	0.54	0.007	27	0.002	36
919	A	1	H	3	51	53	3.51	24.12	0.33	44	14.55	0.54	0.011	87	0.010	9
919	A	1	H	3	100	102	4	27.49	0.36	38	14.55	0.54	0.010	83	0.008	8
919	A	1	H	3	146	148	4.46	30.65	0.47	8	14.55	0.54	0.003	78	0.002	0
919	A	1	H	4	46	48	4.96	34.08	0.10	73	14.55	0.54	0.006	93	0.005	2

Table 1 (continued).

Site	Hole	Core	Type	Section	Top (cm)	Bottom (cm)	Depth (mbsf)	Bslt MAR (g/cm^2/k.y.)	CS %Grnt ("granite" abundance in terrigenous coarse-sand fraction)	Grnt MAR (g/cm^2/k.y.)	CS %CGBs ("coarse-grained basic" abundance in terrigenous coarse-sand fraction)	CGBs MAR (g/cm^2/k.y.)	CS %Sed (sedimentary rock fragment abundance in terrigenous coarse-sand fraction)	Sed MAR (g/cm^2/k.y.)	CS %Carb (carbonate rock fragment abundance in terrigenous coarse-sand fraction)	Carb MAR (g/cm^2/k.y.)
919	A	1	H	1	55	57	0.55	0	17	0	0	0	0	0	0	0
919	A	1	H	1	100	102	1	0	5	0	0	0	0	0	0	0
919	A	1	H	1	144	146	1.44	0.008	5	0.022	2	0.008	26	0.115	0	0
919	A	1	H	2	51	53	2.01	0	7	0.002	0	0	0	0	0	0
919	A	1	H	2	99	101	2.49	0.002	7	0.002	5	0.001	0	0	0	0
919	A	1	H	2	140	142	2.9	0.002	36	0.002	0	0	0	0	0	0
919	A	1	H	3	51	53	3.51	0.001	4	0	0	0	0	0	0	0
919	A	1	H	3	100	102	4	0	8	0	0	0	0	0	0	0
919	A	1	H	3	146	148	4.46	0	11	0	0	0	11	0	0	0
919	A	1	H	4	46	48	4.96	0	5	0	0	0	0	0	0	0

Notes: Sed Rate = sedimentation rate; DBD = dry bulk density; IRD MAR = ice-rafted debris mass accumulation rate; Qtz MAR = quartz mass accumulation rate; Bslt MAR = basalt mass accumulation rate; Grnt MAR = granite mass accumulation rate; CGBs MAR = coarse-grained basic mass accumulation rate; Sed MAR = sedimentary rock fragment mass accumulation rate; Carb MAR = carbonate rock fragment mass accumulation rate.

This is a sample of the table that appears on the volume CD-ROM.

IRD grains, then all grains were counted. Grains were classified as quartz (monocrystalline + polycrystalline grains), basalt (black to dark green, fine-grained igneous grains), granite/coarse-grained acidic (coarse-grained, quartz-bearing, polycrystalline igneous and metamorphic grains), coarse-grained basic/coarse-grained mafic (black to dark green, coarse-grained igneous and metamorphic grains), sedimentary, and sedimentary carbonate. The abundances of each grain type, and the resulting MARs of each IRD grain type, are listed for each sample in Table 1.

RESULTS

The total IRD MARs are listed in Table 1 and are plotted as a function of age in Figure 1. The lithologic composition of the coarse sand-sized IRD and the resultant MARs for each grain type are also listed in Table 1 and are plotted as a function of age in Figures 2, 3, 4, 5, and 6.

The total MARs of coarse-sand IRD (Fig. 1) range from 0 to ~0.50 g/cm^2/k.y., with large amplitude fluctuations primarily older than 250 ka. The distribution of peaks in the IRD MAR profile suggests cyclic variations in IRD supply, with periodicity on the order of 40–100 k.y. The details of this cyclicity will be investigated further by future correlation with an isotopically based time scale.

Quartz, basalt, and granite/coarse-grained acidic are the most abundant IRD grain types at Site 919; MARs of quartz IRD range from 0 to 0.25 g/cm^2/k.y. (Fig. 2), MARs of basalt IRD range from 0 to 0.19 g/cm^2/k.y. (Fig. 3), and MARs of granite/coarse-grained acidic IRD range from 0 to 0.10 g/cm^2/k.y. (Fig. 4). With the exceptions of a few single-point peaks, the MARs of coarse-grained basic IRD and sedimentary rock fragment IRD are low throughout Site 919 (Figs. 5, 6).

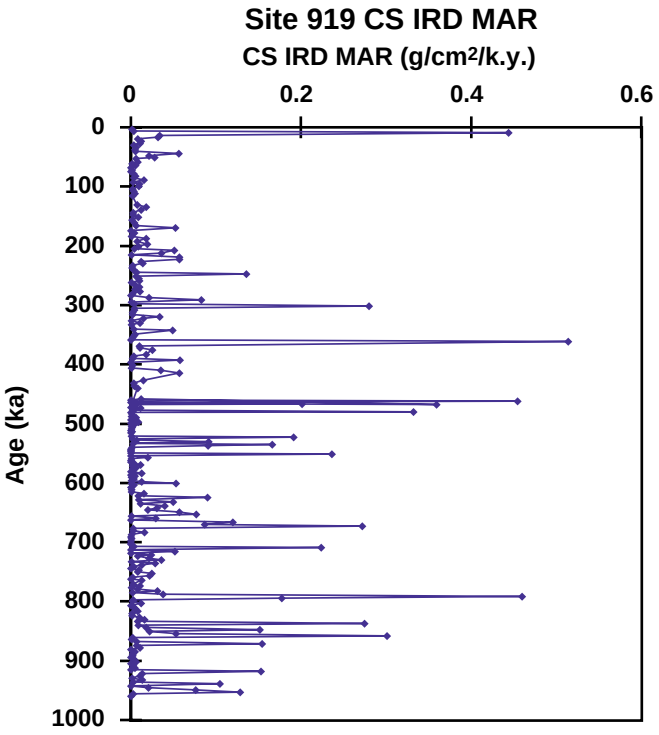

Figure. 1. Total mass accumulation rates (MAR) of terrigenous coarse sand-sized ice-rafted debris (IRD) at Site 919, plotted as a function of age. The distribution of peaks suggests relatively cyclic variations in IRD supply, with most of the large supply events prior to ~250 ka.

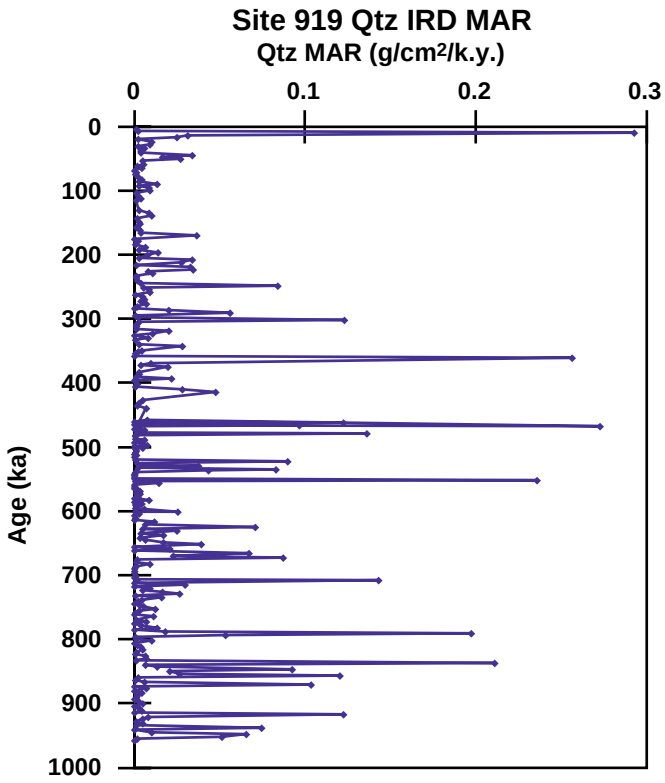

Figure 2. Mass accumulation rates (MAR) of coarse sand-sized quartz ice-rafted debris (IRD) at Site 919, plotted as a function of age.

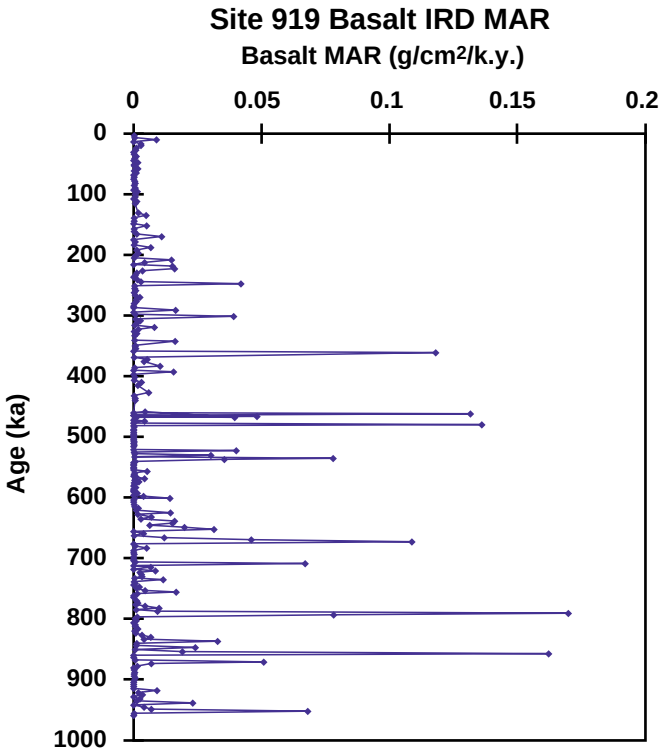

Figure 3. Mass accumulation rates (MAR) of coarse sand-sized basaltic ice-rafted debris (IRD) at Site 919, plotted as a function of age.

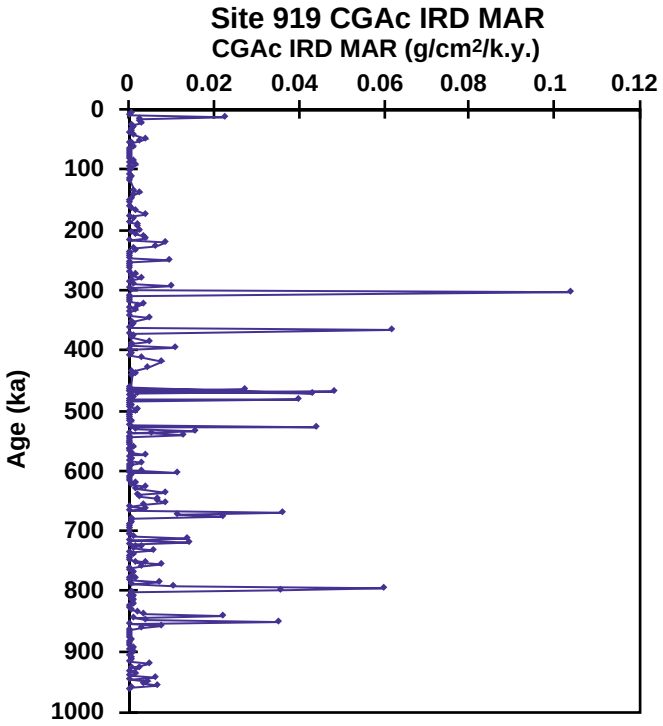

Figure 4. Mass accumulation rates (MAR) of coarse sand-sized granitic (or coarse-grained acidic, CGAc) ice-rafted debris (IRD) at Site 919, plotted as a function of age.

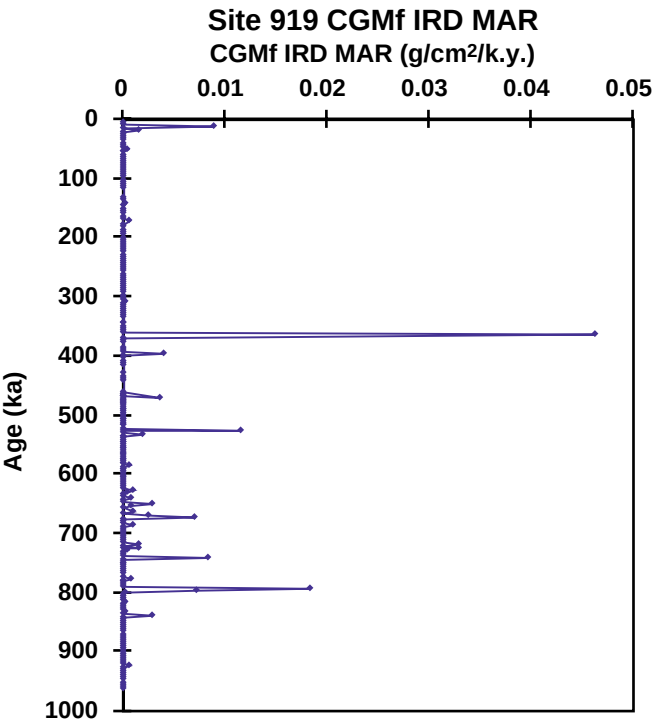

Figure 5. Mass accumulation rates (MAR) of coarse sand-sized coarse-grained basic (or coarse-grained mafic, CGMf) ice-rafted debris (IRD) at Site 919, plotted as a function of age.

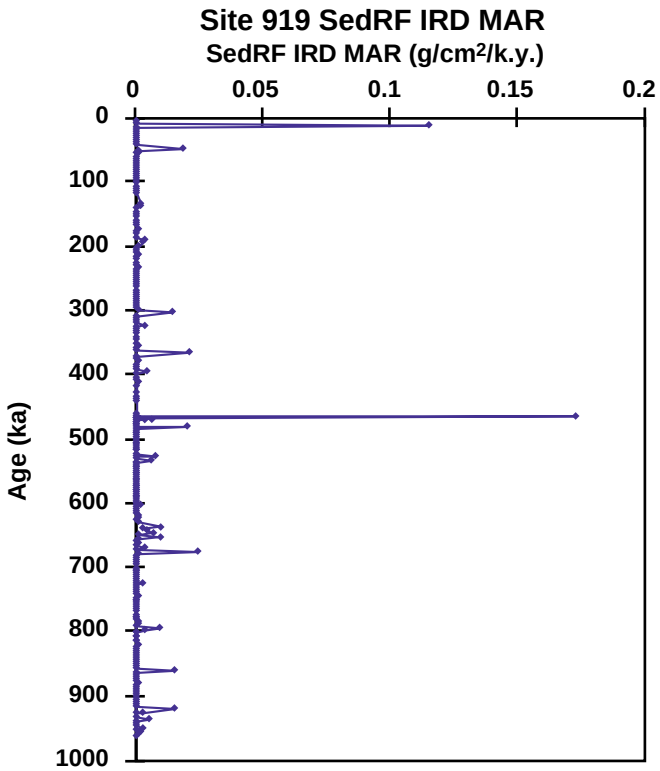

Figure 6. Mass accumulation rates (MAR) of coarse sand-sized sedimentary rock fragment ice-rafted debris (IRD) at Site 919, plotted as a function of age.

Peaks in the profile of total IRD MARs (Fig. 1) generally result from increases in the MARs of both quartz and basalt IRD (Figs. 2, 3), suggesting that IRD supply from at least two geographically and geologically distinct source regions varied synchronously through the Pleistocene. Future work will compare these compositional characteristics with those from nearby Site 918 in order to determine the relative effects of regional glacial histories and iceberg dispersal patterns on the histories of IRD MARs.

ACKNOWLEDGMENTS

Walter Hale and his staff at the core repository in Bremen, Germany, provided efficient and able assistance with sampling. Attiya Mobin-Uddin, Jessica Albrecht, Maura Metheny, and Chris Brown assisted with sample processing. Sam Boggs, Jr., provided a helpful review of the manuscript. This work was funded by a JOI-USSSP postcruise grant (Leg 163); this support is gratefully acknowledged.

REFERENCES

Bond, G., Heinrich, H., Huon, S., Broecker, W., Labeyrie, L., Andrews, J., McManus, J., Clasen, S., Tedesco, K., Jantschik, R., Simet, C., and Klas, M., 1992. Evidence for massive discharges of icebergs into the glacial North Atlantic. *Nature*, 360:245–249.

Conolly, J.R., and Ewing, M., 1970. Ice-rafted detritus in northwest Pacific deep-sea sediments. *In* Hayes, J.D. (Ed.), *Geological Investigations of the North Pacific*. Mem. Geol. Soc. America, 126:219–231.

Flower, B.P., 1998. Mid- to late Quaternary stable isotopic stratigraphy and paleoceanography at Site 919 on the southeast Greenland margin. *In* Saunders, A.D., Larsen, H.C., Wise, S.W., Jr., et al., *Proc. ODP, Sci. Results*, 152: College Station, TX (Ocean Drilling Program).

Goldschmidt, P.M., 1995. Accumulation rates of coarse-grained terrigenous sediment in the Norwegian-Greenland Sea: signals of continental glaciation. *Mar. Geol.*, 128:137–151.

Greenland Ice-Core Project (GRIP) Members, 1993. Climate instability during the last interglacial period recorded in the GRIP ice core. *Nature*, 364:203–207.

Jansen, E., Sjoholm, J., Bleil, U., and Erichsen, J.A., 1990. Neogene and Pleistocene glaciations in the Northern Hemisphere and late Miocene–Pliocene global ice volume fluctuations: evidence from the Norwegian Sea. *In* Bleil, U., and Thiede, J. (Eds.), *Geological History of the Polar Oceans: Arctic versus Antarctic:* Dordrecht (Kluwer Academic), 677–705.

Krissek, L.A., 1989. Late Cenozoic records of ice-rafting at ODP Sites 642, 643, and 644, Norwegian Sea: onset, chronology, and characteristics of glacial/interglacial fluctuations. *In* Eldholm, O., Thiede, J., et al., *Proc. ODP, Sci. Results*, 104: College Station, TX (Ocean Drilling Program), 61–4.

————, 1995. Late Cenozoic ice-rafting records from Leg 145 sites in the North Pacific: late Miocene onset, late Pliocene intensification, and Pliocene-Pleistocene events. *In* Rea, D.K., Basov, I., Scholl, D.W., Allen, J., et al., *Proc. ODP, Sci. Results*, 145: College Station, TX (Ocean Drilling Program).

Larsen, H.C., Saunders, A.D., Clift, P.D., et al., 1994. *Proc. ODP, Init. Repts*., 152: College Station, TX (Ocean Drilling Program).

Ruddiman, W.F., 1977. Late Quaternary deposition of ice-rafted sand in the subpolar North Atlantic (lat 40° to 65°N.). *Geol. Soc. Am. Bull*., 88:1813–1827.

Date of initial receipt: 5 January 1998
Date of acceptance: 15 May 1998
Ms 163SR-118